Available online at www.sciencedirect.com
ScienceDirect
Polymer 49 (2008) 1547–1554
polymer
www.elsevier.com/locate/polymer

Cadmium selenide nanowires within core–shell cylindrical polymer brushes: Synthesis, characterization and the double-loading process

Jiayin Yuan, Markus Drechsler, Youyong Xu, Mingfu Zhang, Axel H.E. Müller*

Makromolekulare Chemie II and Bayreuther Zentrum für Kolloid- und Grenzflächenforschung, Universität Bayreuth, D-95440 Bayreuth, Germany

Received 3 December 2007; received in revised form 17 January 2008; accepted 21 January 2008
Available online 2 February 2008

Abstract

Cadmium selenide (CdSe) nanowires were successfully in situ fabricated, utilizing amphiphilic core–shell cylindrical polymer brushes (CPB) as well-defined single molecular templates. The hydrophilic polymer brush core acts as the nanoreactor for generating and shaping CdSe nanoparticles into nanowires via the absorption of cadmium ions by carboxylate groups in the core and subsequent introduction of H_2Se gas; the hydrophobic polymer brush shell protects the nanowires from agglomeration and renders the hybrid a soluble material. The formation of 170 nm-long CdSe nanowires proceeds simultaneously with the nucleation, growth and combination of CdSe nanoparticles. After the introduction of CdSe nanowires, the recuperated chemical structure of CPB facilitates a double-loading process, broadening the CdSe nanowire from 7.5 to 9.3 nm on an average. Both hybrids are soluble and stable in organic solvents for one year and a potential candidate of the nanoscale optic and electronic devices.

Keywords: Cadmium selenide; Semiconductors; Nanowires

1. Introduction

Semiconductor nanowires [1–6] are considered as the prospective building blocks, interconnects and functional components for assembling nanosized photonic, electronic and optical devices and sensors [7–14]. Among them, cadmium selenide (CdSe) nanowires are promising candidates to build up optoelectronic devices, such as solar cells, and have received steadily growing interest. This has benefited from intensive studies on CdSe quantum dots [15–17]. In the last decade, there have been many efforts to develop CdSe nanowires utilizing a variety of techniques. For instance, direct-current electrodeposition in porous anodic aluminum oxide templates has been used by the groups of Guo [18] and Peng [19] to generate CdSe nanowire with well-controlled crystalline and polycrystalline structure. Lieber and co-workers reported a laser-assisted catalytic growth method to fabricate CdSe nanowires [4]. A surfactant-assisted solution synthesis of CdSe nanowires was published by Rao et al. [20]. The group of Kuno has grown straight and branched CdSe nanowires with lengths between 1 μm and 10 μm by a solution–liquid–solution technique using gold/bismuth core–shell nanoparticles as seeds [21–23]. Chen and co-workers fabricated single-crystalline CdSe nanowires by a chemical vapor deposition method assisted with laser ablation [24]. Xia and co-workers employed the cation-exchange reaction between Ag^+ and Cd^{2+} to transform single-crystal Ag_2Se nanowires into single-crystal CdSe nanowires [25]. A vapor-phase growth of CdSe nanowires assisted with silicon powder was achieved by the group of Zhang [26]. Wang and Ma provided a systematic study on the growth of 1-dimensional CdSe nanostructures by a vapor–liquid–solid process [27]. Great progress until now have been reached, however, the generation of well-distributed and aligned semiconductor nanowires is still challenging in this field.

In addition, polyelectrolytes and biopolymers, like DNA and viruses, have been widely exploited as templates for

* Corresponding author. Tel.: +49 921 553399; fax: +49 921 553393.
E-mail address: axel.mueller@uni-bayreuth.de (A.H.E. Müller).

0032-3861/$ - see front matter © 2008 Elsevier Ltd. All rights reserved.
doi:10.1016/j.polymer.2008.01.063

mineralization and fabrication of various inorganic nanowires due to the mild synthetic conditions [28–32]. However, only a few reports were related to the polymer template-directed synthesis of semiconductor nanowires, with notable examples including micro channels within a thin polymer film [33], a polymer-assisted solvothermal process [34–36], mesoscale structures self-assembled from AB or ABC block copolymers [37,38], and biopolymers such as DNA strains [39,40].

Recently, we reported the formation of wormlike cadmium sulfide (CdS) nanowires within well-defined amphiphilic core–shell cylindrical polymer brushes (CPB) [41]. In this paper, extending this technique, we accomplished the synthesis of CdSe semiconductor nanowires and carried out a double-loading to broaden these nanowires. Comparing the rigorous conditions such as high temperature, high pressure, toxic organometallic precursors, this facile and environmentally benign synthesis using nontoxic reactants appears to be superior.

2. Experimental section

2.1. Materials

All chemicals were of analytical grade and used as received without further purifications. Cadmium acetate dihydrate ($CdAc_2 \cdot 2H_2O$) was purchased from Merck. Selenium powder (<325 mesh, 99.7%) and chloroform (>99.8%, stabilized with amylene) were purchased from Acros. Methanol (>99.8%) and paraffin oil were purchased from Fluka. The CPB $[AA_{25}-nBA_{61}]_{1500}$ (1500 side chains, each consisting of 25 acrylic acid units and 61 *n*-butyl acrylate units, $L_n = 166$ nm, $L_w = 180$ nm) that we used as template was synthesized as reported earlier [42].

2.2. Synthesis of the hybrid of polymer brush and CdSe nanoparticles

Polymer brush, $[AA_{25}-nBA_{61}]_{1500}$ (40.0 mg, containing 0.102 mmol of carboxylic acid groups) was dissolved in 40 mL of a mixture of methanol and chloroform (v/v = 1/1). Then 0.097 mmol of NaOH (0.128 M solution in methanol) was added to neutralize 95% of the carboxylic acid groups. After stirring for 6 h, 0.051 mmol of $CdAc \cdot 2H_2O$ (0.0720 M solution in methanol) was injected and the reaction mixture was stirred for 12 h.

To remove the uncoordinated Cd^{2+} ions, continuous dialysis was carried out in a mixture of methanol and chloroform (v/v = 1/1) using PVDF membrane tubes (MWCO = 500,000, SpectraPor). The process was monitored by the conductivity change of the dialyzate measured with an automatic titration system (Titrando 809, Metrohm) and ended when an almost constant conductivity was obtained during the dialysis.

The formation of CdSe particles was carried out under argon atmosphere. A three-neck round bottom flask charged with a stirring bar, thermometer, condenser, 2.0 g of selenium powder and 50 ml of paraffin oil was bubbled by argon for half an hour and then heated to 300 °C under vigorous stirring [43]. The mixture became a dark red clear solution above 220 °C due to the melting of the Se powder (mp = 217 °C). The released H_2Se gas was distributed by argon flow through the glass pipeline into the polychelate solution. The reaction mixture turned red instantly, signifying the formation of CdSe nanoparticles. After 1 h the obtained transparent dark red solution was bubbled with Ar for 1 h, degassed by three cycles of freeze-pump-thaw process and diluted to 100 ml. This solution was ready for double-loading process in an analogous procedure.

2.3. Characterization

Atomic force microscopy (AFM) images were recorded on a Digital Instruments Dimension 3100 microscope operated in tapping mode with minimum amplitude setpoint to avoid strong deformation of the objects. The samples were prepared by dip-coating from dilute sample solutions in a mixture of methanol/chloroform (v/v = 1/1) onto freshly cleaved mica. The height profile analysis was conducted with Nanoscope III and Uthscsa Image Tool software.

Transmission electron microscopy (TEM) images were taken on a Zeiss/LEO 922 OMEGA microscope operated at 200 kV, or a Zeiss CEM 902 microscope operated at 80 kV. To prepare the samples, 1 μL of a dilute solution of 0.01 g/L (polymer content) was put onto a copper grid (300 mesh, Plano) coated with a SiO_x film and dried in the saturated solvent vapor at ambient temperature. Energy-dispersive X-ray (EDX) analysis was performed on a LEO 1530 field emission scanning electron microscope using an X-ray detector. The samples were obtained similarly except onto a silicon wafer.

UV–vis absorption spectra of samples in methanol/chloroform (v/v = 1/1) were recorded on a Perkin–Elmer Lambda 15 UV–vis spectrophotometer. Photoluminescence spectra of samples were collected on a Shimadzu RF-5301 PC spectrofluorometer.

3. Results and discussion

A general approach employing CPBs as templates to fabricate CdSe nanowires includes three steps as shown in Scheme 1, similar as we reported before. In the first step (a to b), the carboxylic groups in the poly(acrylic acid) (PAA) core were neutralized by NaOH. Via ion exchange, Cd^{2+} ions replace Na^+ ions (step 2: b to c), forming a polychelate [44]. The purified polychelate solution reacted with H_2Se gas to generate CdSe nanoparticles aligned within the cylindrical core (step 3: c to d). Simultaneously, the PAA core resumes the initial chemical structure (i.e., acrylic acid functions) which enables the double-loading process by repeating steps 1–3.

The CPB $[AA_{25}\text{-}nBA_{61}]_{1500}$ as a unimolecular template with a low length polydispersity ($L_w/L_n = 1.08$) [42], as visualized by AFM in Fig. 1A, defines both the dimension and size distribution of the CdSe nanowires within the core region. The wormlike cylinders are distinctly visible in the height image, whereas the core–shell structure is seen in the phase image. After the uptake of Cd^{2+} the characteristic "pearl necklace" [45] morphology is identified by AFM images in Fig. 1B due to the "cross-linking" of side chains initiated by the

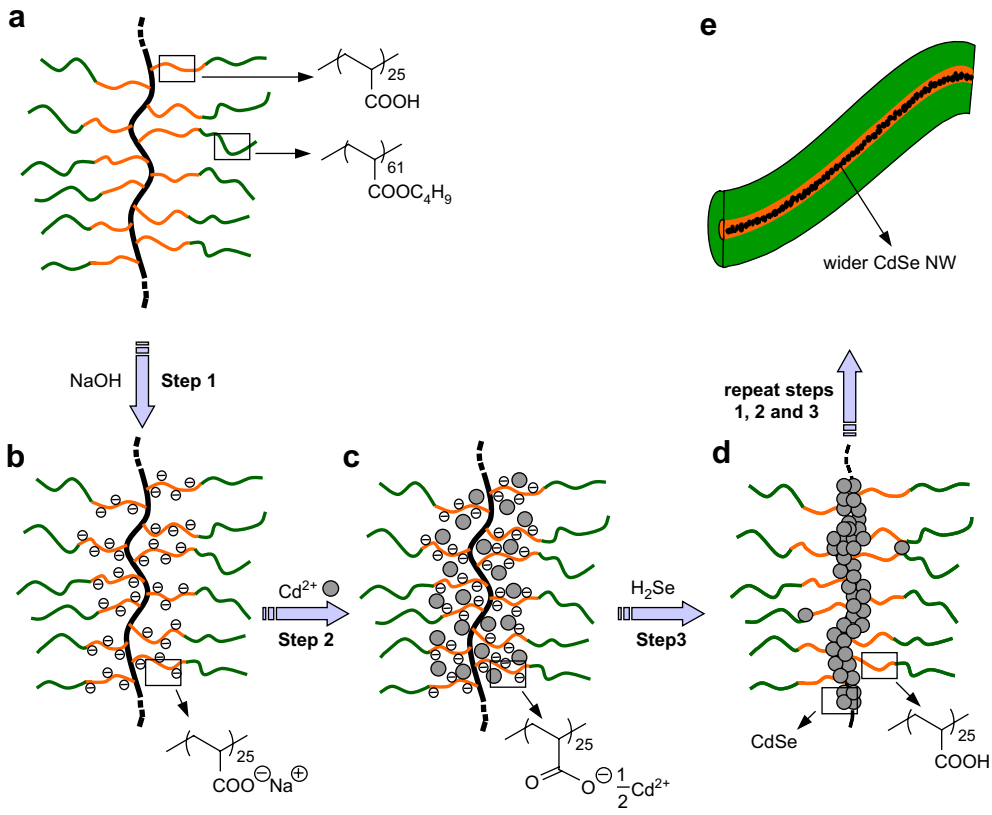

Scheme 1. Illustration of the CdSe nanowire synthesis inside the CPB: (a) the core–shell CPB, $[AA_{25}–nBA_{61}]_{1500}$; (b) neutralized polymer brush with poly(sodium acrylate) core; (c) polychelate of the polymer brush and Cd^{2+}; (d) the first loaded hybrid of the CPB and CdSe nanowires and (e) the second loaded hybrid of the CPB and CdSe nanowires.

coordination between divalent Cd^{2+} ions and monovalent carboxylate groups from different side chains [41]. To elaborate this change, the longitudinal height profile of single brush is analyzed in Fig. 1, in which the CPB (Fig. 1A, right) possesses a relatively lower height and smoother contour in contrast to the polychelate (Fig. 1B, right). The results from the height profile analysis, as summarized in Table 1, ensures that the chelation of Cd^{2+} ions and carboxylic groups remarkably increases the average height from 0.71 nm of the CPB to 2.40 nm of the polychelate, and the standard deviation reflecting the inhomogeneity in the brush height shifts from 0.20 of the CPB to 1.00 of the polychelate.

Transmission electron microscopy (TEM) does not give a clear image of the pure polymer brushes due to the rather low contrast. The chelation with Cd^{2+} enhances the visibility. Fig. 2 shows wormlike dark grains (7–13 nm) oriented within the CPB. A zoom portrays a string of dark dots, which supports the "pearl necklace" structure of the polychelate verified by AFM in Fig. 1B. The "pearl necklace" structure vanishes after reaction of H_2Se with Cd^{2+}, forming the hybrid, as shown in the AFM image in Fig. 3A. The reason is that although the coordinated Cd^{2+} ions in the polychelate are confined separately, in situ produced CdSe can diffuse, form nuclei and grow into a continuous phase due to the forfeit of the strong ionic bond between Cd^{2+} and the carboxylic acid groups. As shown in Table 1, the average height of the polychelates (2.40 nm) retracts to 2.00 nm of the hybrid brush, but still 1.30 nm higher than that of the pure CPB. Meanwhile the standard deviation of the hybrid decreases from 1.00 of the polychelate to 0.64, but remains higher than 0.20 of the CPB. Thus, the hybrid molecules are relatively "flatter" than the polychelate, but rougher than the CPB. Since the carboxylic acid coordination sites after the formation of CdSe nanowires were resumed, the reloading of CdSe nanoparticles was subsequently carried out in the same manner. The hybrid polychelate, named after the combination of the hybrid and the coordinated Cd^{2+} ions exhibits again the "pearl necklace" morphology in the AFM images in Fig. 3B, although not as obvious as in the polychelate. Its height average (see Table 1) increases from 2.0 nm of the hybrid, to 3.3 nm, and is 0.9 nm higher than that of the polychelate, because of the overlapped size-expansion effects from the formed CdSe nanowires and the crosslinking caused by newly introduced Cd^{2+}. The standard deviation of the hybrid polychelate increases to 0.90, a little lower than 1.00 of the polychelate, since the deformation caused by the coordination is partially prevented by the solid CdSe nanowire inside the brush core. After reaction of the reloaded Cd^{2+} with H_2Se, the double-loaded hybrid shrinks to 2.66 nm, higher than 2.00 of the first loaded one, which insinuates a further size expansion of the polymer brush as a result of the double-loading. Yet it unexpectedly shows the highest standard deviation, which may indicate that the new CdSe nanoparticles render the shape of the nanowires more irregular.

Fig. 3D shows a representative TEM image of the first loaded hybrid of the polymer brush and the CdSe nanowires.

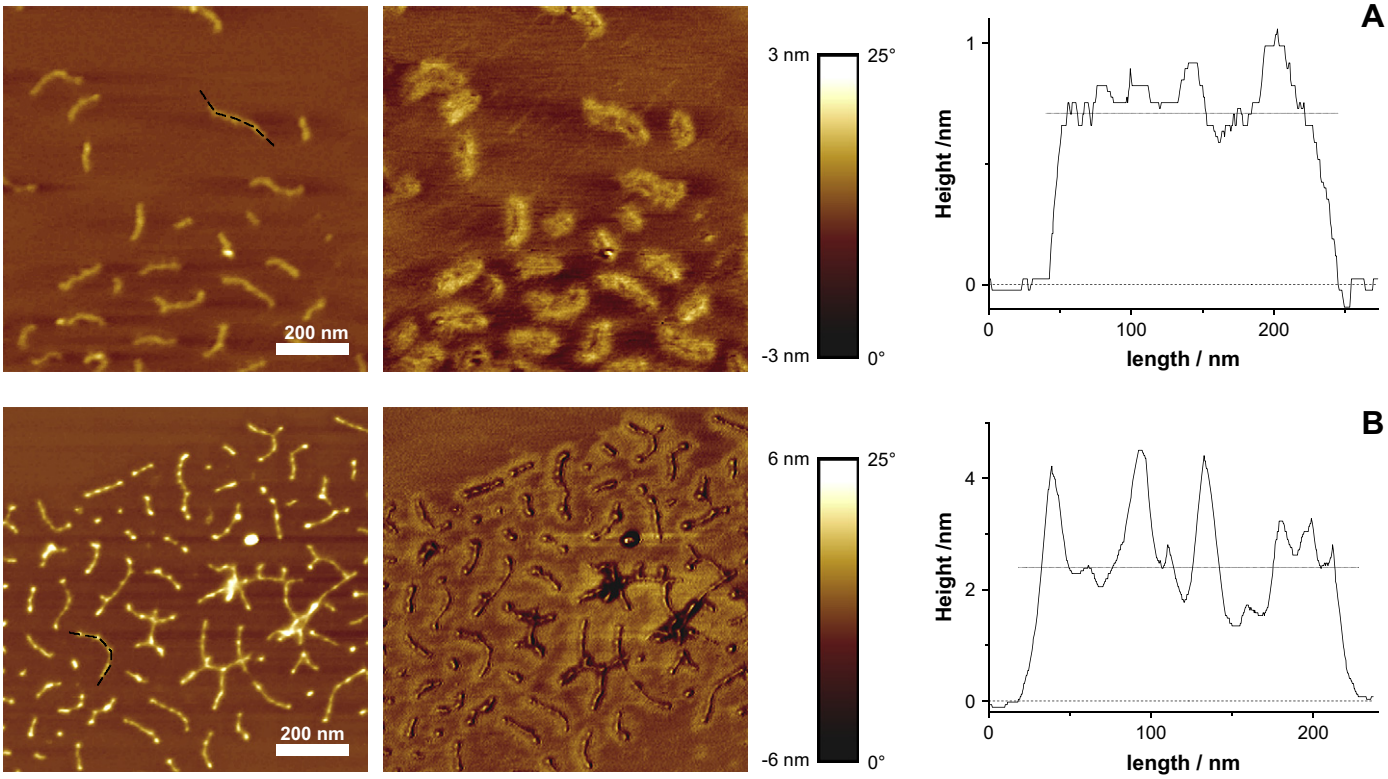

Fig. 1. Tapping mode AFM images (left, height; right, phase) and height profile of a single brush marked by the black dash line in (A) the core–shell CPB, $[AA_{25}-nBA_{61}]_{1500}$; (B) the polychelate of the CPB and Cd^{2+} ions (average height is indicated by the dotted line).

Table 1
Height profile analysis of single brushes in AFM images of (A) the core–shell CPB, $[AA_{25}-nBA_{61}]_{1500}$; (B) the polychelate; (C) the first loaded hybrid; (D) the hybrid polychelate; and (E) the double-loaded hybrid

Samples	Average height/nm	Standard deviation/nm
A	0.71	0.20
B	2.40	1.00
C	2.00	0.64
D	3.30	0.90
E	2.66	1.44

In contrast to the polychelate in Fig. 2, a higher contrast was attained due to the formation of CdSe nanoparticles. To characterize the width of the CdSe nanowires, a statistical calculation was performed by measuring the nanowire width at different locations away from the distorted joints. The result in Fig. 3G stands for a quasi-Gaussian monomodal distribution curve where the widths range from 5 to 11 nm with an average value of 7.6 nm. After reloading Cd^{2+} ions into the hybrid to form the hybrid polychelate, the nanowires show big "knobs" along their backbone, as shown in Fig. 3E. As we have discussed above, the polychelate Cd^{2+} ions coordinate with the carboxylic

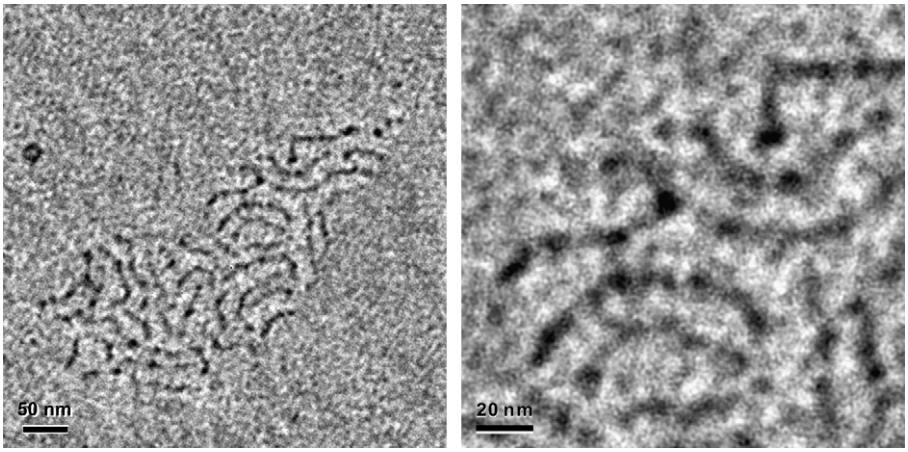

Fig. 2. Non-stained TEM images of the polychelate of the core–shell CPB $[AA_{25}-nBA_{61}]_{1500}$ and Cd^{2+} ions. The right image is the enlarged view of the left one.

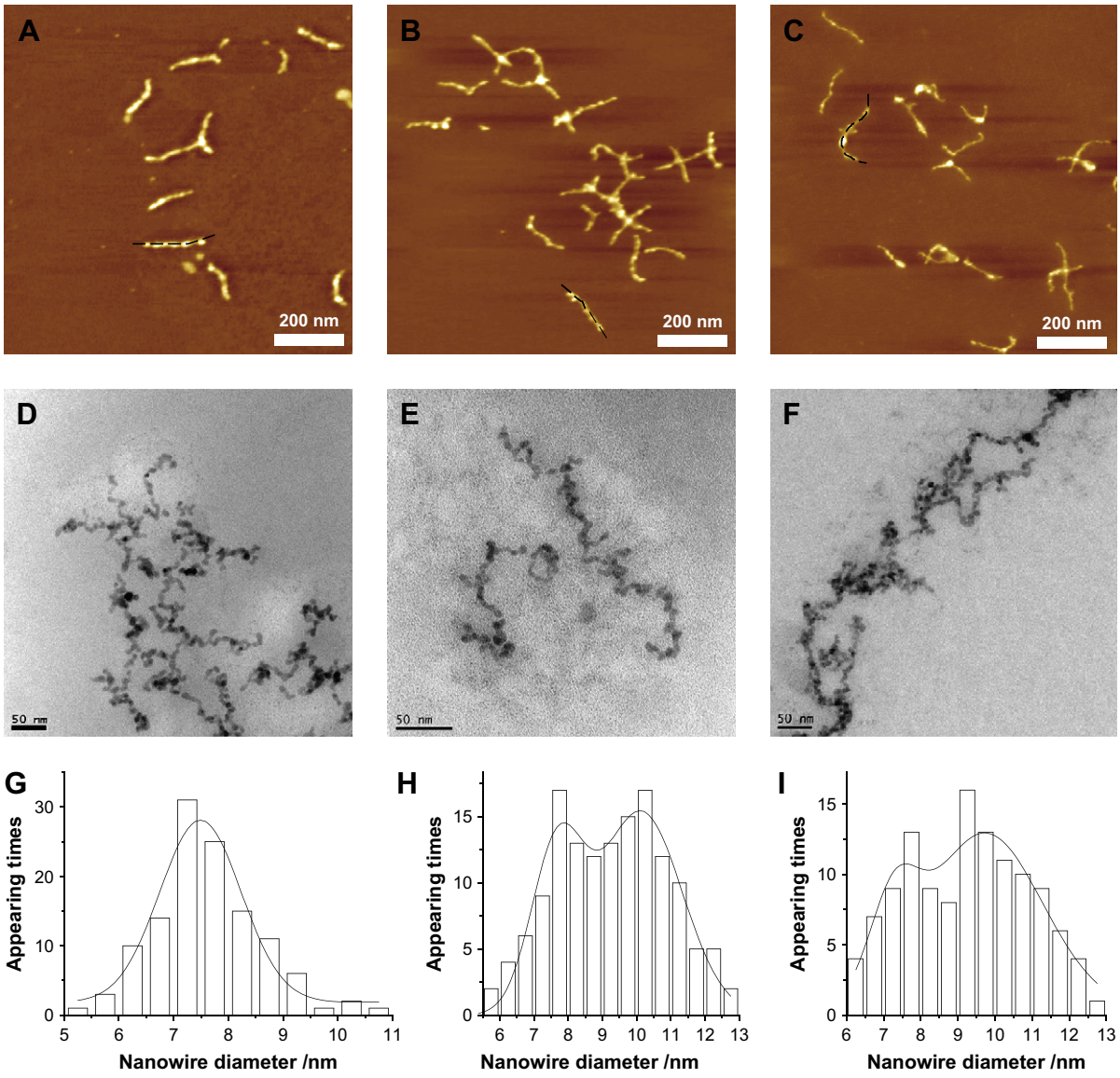

Fig. 3. (A–C) Tapping mode AFM height images of (A) the first loaded hybrid of the core–shell CPB $[AA_{25}-nBA_{61}]_{1500}$ and CdSe nanowires (*Z* range: 6 nm), (B) the hybrid polychelate of the first loaded hybrid and Cd^{2+} ions (*Z* range: 12 nm) and (C) the double-loaded hybrid of the polymer brush and CdSe nanowires (*Z* range: 12 nm). The single polymer brushes/hybrids in each image marked with a black dash line were used for the height analysis in Table 1, (D–F) corresponding non-stained TEM images and (G–I) statistic width distributions of the nanowire diameters in the corresponding TEM images.

groups on different side chains to form the separated necklace-like spheres; in the case of the hybrid polychelates, the already existing CdSe nanowire connects the isolated necklace-like spheres after the reloading of Cd^{2+} ions. In the corresponding width distribution curve (Fig. 3H), the hybrid polychelates show a bimodal distribution. The first peak between 7 and 8 nm stands at the same position as the peak in Fig. 3G, while the second peak appears around 10 nm standing for the protrusion due to the spheres along the nanowires. The reloading of CdSe nanoparticles to CdSe nanowires is completed by bubbling H_2Se to the hybrid polychelate solution. Fig. 3F shows a TEM image of the double-loaded hybrid, in which the linear CdSe nanowires are clear to see. The statistic width calculation in Fig. 3I demonstrates a bimodal quasi-Gaussian distribution and an average of 9.3 nm similar to that of the hybrid polychelate, which reveals that the newly formed CdSe nanoparticles in the spheres of the hybrid polychelate are almost directly attached to the nearby CdSe nanowire surface.

In order to understand the crystalline structure, selected area electron diffraction (SAED) was applied to the first loaded hybrid, the hybrid polychelates and the double-loaded hybrid, all of which show a polycrystalline behavior. The SAED rings of the first loaded hybrid are presented in Fig. 4A. It supports the presence of polycrystalline particles, which often appears in template-directed methods. The *d* spacings calculated from the rings are 3.51, 2.15, and 1.83 Å, which correspond to the lattice planes [111], [220], and [311] of the cubic (zinc blende) phase of CdSe (Joint Committee on Powder Diffraction Standards file No. 19-0191). Since the SAED pattern represents the collective behavior of the crystallites, the intrinsic structure of CdSe nanowire is further examined by high resolution TEM (HRTEM) in Fig. 4B. The lattice plane with an interplanar

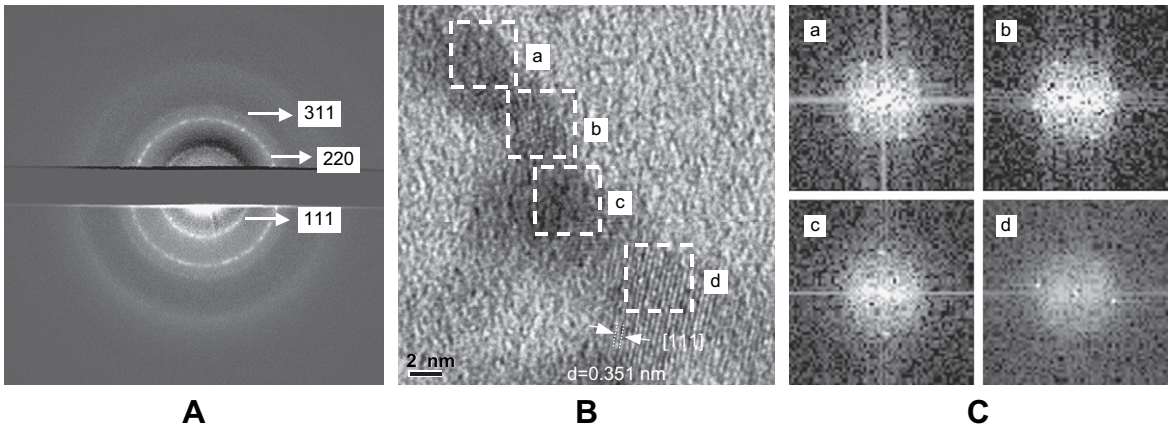

Fig. 4. (A) SAED pattern of the hybrid of the core–shell CPB $[AA_{25}–nBA_{61}]_{1500}$ and CdSe nanowires (image subtracted by the blank grid), (B) HRTEM image of the crystals aligned along the CdSe nanowires, and (C) Fast Fourier Transform (FFT) pattern corresponding to the white squares in HRTEM image in (B).

distance of 0.351 nm corresponding to the [111] plane was directly observable in square *d*. The same lattice planes in other areas of the nanowires (squares a, b and c) are somewhat smeared but can be detected by the FFT pattern, as shown in Fig. 4C. Every two symmetric and opposite white points define a line, which is perpendicular to the lattice plane. In this way, the differently oriented crystals were found along the nanowires, indicating that the polycrystallinity of the hybrid material actually results from the intrinsic polycrystallinity of each nanowire itself.

Elemental analysis of the hybrids was achieved by the energy-dispersive X-ray (EDX) analysis of a scanning electron micrograph. Fig. 5 shows the EDX spectrum of the second loaded hybrid of the polymer brush and CdSe nanowires on a silicon wafer, which confirms the presence of cadmium and selenium. The collected EDX results of the two hybrids in Table 2 present the ratios of Cd to Se close to the theoretical value. If the amount of polymer is calculated from the carbon content (Fig. 5), and the CdSe from the sum of Cd and Se content, 21.9% and 38.2% of CdSe were embedded in the first and second loaded hybrids, respectively (Table 2). Since there is a considerable experimental error due to the weak signals in EDX analysis, we verified the successful introduction of more CdSe nanoparticles during the double-loading process by UV–vis spectroscopy.

In Fig. 6, the weak UV–vis absorption of the polychelate supports that the strong absorption of the two hybrids comes exclusively from CdSe nanowires. The double-loaded hybrid shows stronger absorption than the single-loaded one, confirming the increase of the CdSe amount during the double-loading process. It is known that bulk CdSe starts to absorb at about 716 nm [15]. The first loaded hybrid shows an absorption

Table 2
EDX results of the amount of Cd and Se in the first loaded and double-loaded hybrids

Samples	First loading	Second loading
Cd/Se	1.18	1.08
CdSe content	21.9 ± 5.9%	38.2 ± 7.2%

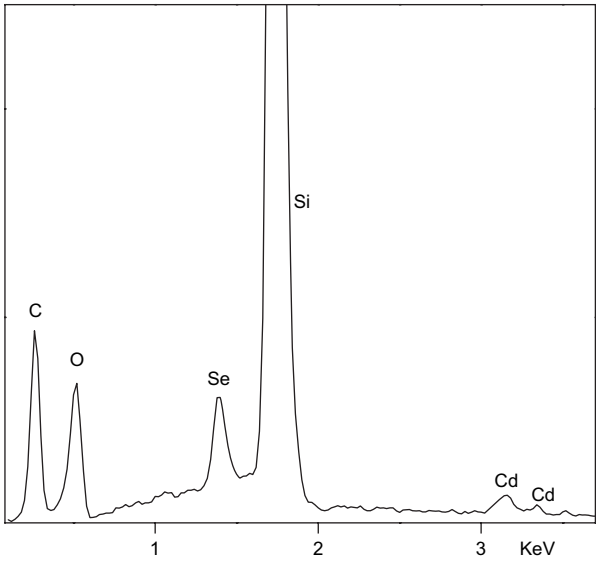

Fig. 5. EDX spectrum of the double-loaded hybrid of the polymer brush and CdSe nanowires.

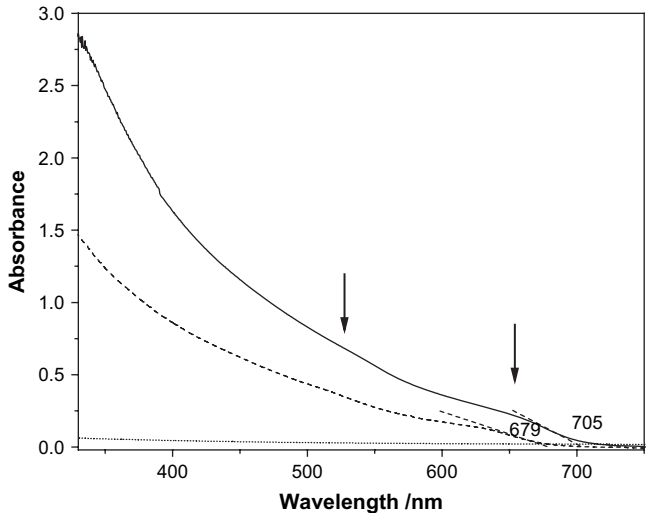

Fig. 6. UV–vis spectra of the polychelate (dotted line), the first loaded hybrid (dashed line) and double-loaded hybrid (solid line), the concentration for all is 0.4 g/L (polymer content).

onset at 679 nm and the double-loaded one at 705 nm. Both display a blue-shift relative to that of bulk CdSe, indicating the existence of the quantized transition. According to Murray's empirical curve [15], the threshold corresponds to CdSe nanoparticles with a rough size of 7 nm and 10 nm, respectively, which proves the growth of CdSe nanowires by width during the double-loading process. These values are close to the nanowire average width values of 7.6 and 9.3 nm as obtained by TEM, which indicates that the quantized effect of the nanowire detected according to the blue-shift of the absorption edge most probably arises from the width of the nanowires. Besides, a weak transition for both hybrids at around 550 nm is observed, corresponding to a nanoparticle size of roughly 3 nm, which becomes more obvious at higher concentration. The existence of multi-absorption transitions confirms the TEM analysis because the nanowires are constructed by a linear interconnection of differently sized CdSe nanocrystals, which are probably a fusion of two or more even smaller nanoparticles during the nanowire formation process. AFM images support this because the height of the CdSe nanowires is limited to the maximum height of the hybrid molecules in Table 1. The first loaded hybrid showed a maximum height of 3.38 nm and the second one of 7.30 nm, both are smaller than the width of the nanowires and the nanoparticle size deduced from the UV threshold absorptions. This, in essence, leads to the flat shape of the nanowires, which are around 2 nm high and 7.5 nm wide for the first loaded hybrid, and 2.66 nm high and 10.5 nm wide for the second one. Besides, the CdSe nanoparticles which were in situ formed in the polymer brush core and failed to reach the CdSe nanowires also contribute to the absorption at higher energies.

The photoluminescence (PL) behavior of both hybrids shows an unusual dependence on the excitation wavelength. For example, a lower excitation wavelength results in a blue-shifted wide emission. This can be understood, since the whole nanowire is created by the alignment and connection of different sized and random oriented CdSe nanocrystals, thus a lower excitation wavelength is able to excite smaller sized nanocrystals. Moreover the aligned CdSe nanocrystals are more similar to the close-packed quantum dots rather than the usual isolated nanocrystals embedded in polymer matrix. In such case, the electronic energy transfer between the small and large quantum dots is involved through the dipole–dipole interdot interactions [46–51]. Furthermore, very recently the PL intensity heterogeneity along the length of individual nanowires due to all kinds of disorder like surface/interface roughness and so on, was also reported by Kuno et al. [52], which suggests that the photoluminescence of the nanowires is governed not only by the building block like nanocrystals, but also by the disorder caused fluctuations of the exciton potential along the nanowire.

4. Conclusion

CdSe nanowires were successfully fabricated using well-defined core–shell amphiphilic cylindrical polymer brushes with PAA core and P*n*BA shell as unimolecular templates under mild solution conditions. The products were characterized by AFM, TEM, EDX, UV–vis and photoluminescence spectroscopies. A double-loading of CdSe nanoparticles into the polymer brush core was carried out and its influence was examined in detail. The double-loading presents the unique advantage of the polymer brushes as both nanoreactor and template. The hybrids from both loadings showed good solubility and stability (one year without any precipitation) in a concentration below 0.4 g/L. The single CdSe nanowires protected by the polymer brush shell can be handled in solution and serve as a candidate for electronic nanoscale devices.

Acknowledgement

This work was financially supported by Deutsche Forschungsgemeinschaft (DFG) within Priority Program SPP 1165 (Mu896/22-2). We thank Ms. Violetta Olszowka and Mr. Markus Hund for their help in AFM analysis.

References

[1] Lieber CM. MRS Bull 2003;28:486.
[2] Yang P. MRS Bull 2005;30:85.
[3] Teo BK, Sun XH, Hung TF, Meng XM, Wong NB, Lee ST. Nano Lett 2003;3:1735.
[4] Duan X, Lieber CM. Adv Mater 2000;12:298.
[5] Li Q, Gong X, Wang C, Wang J, Ip K, Hark S. Adv Mater 2004;16:1436.
[6] Hu J, Bando Y, Liu Z, Sekiguchi T, Golberg D, Zhan J. J Am Chem Soc 2003;125:11306.
[7] Kim H-M, Cho Y-H, Lee H, Kim SI, Ryu SR, Kim DY, et al. Nano Lett 2004;4:1059.
[8] Johnson JC, Choi H-J, Knutsen KP, Schaller RD, Yang P, Saykally RJ. Nat Mater 2002;1:106.
[9] Greytak AB, Barrelet CJ, Li Y, Lieber CM. Appl Phys Lett 2005;87:151103/1.
[10] Huang Y, Duan X, Lieber CM. Small 2005;1:142.
[11] Sirbuly DJ, Law M, Yan H, Yang P. J Phys Chem B 2005;109:15190.
[12] Holmes JD, Johnston KP, Doty RC, Korgel BA. Science 2000;287:1471.
[13] Wang ZL. Adv Mater 2003;15:432.
[14] Li SY, Lee CY, Lin P, Tseng TY. J Vac Sci Technol B Microelectron Nanometer Struct-Process Meas Phenom 2006;24:147.
[15] Murray CB, Norris DJ, Bawendi MG. J Am Chem Soc 1993;115:8706.
[16] Peng X, Schlamp MC, Kadavanich AV, Alivisatos AP. J Am Chem Soc 1997;119:7019.
[17] Landes C, Burda C, Braun M, El-Sayed MA. J Phys Chem B 2001;105:2981.
[18] Xu D, Shi X, Guo G, Gui L, Tang Y. J Phys Chem B 2000;104:5061.
[19] Peng XS, Zhang J, Wang XF, Wang YW, Zhao LX, Meng GW, et al. Chem Phys Lett 2001;343:470.
[20] Rao CNR, Govindaraj A, Deepak FL, Gunari NA, Nath M. Appl Phys Lett 2001;78:1853.
[21] Khandelwal A, Jena D, Grebinski JW, Hull KL, Kuno MK. J Electron Mater 2006;35:170.
[22] Grebinski JW, Richter KL, Zhang J, Kosel TH, Kuno M. J Phys Chem B 2004;108:9745.
[23] Grebinski JW, Hull KL, Zhang J, Kosel TH, Kuno M. Chem Mater 2004;16:5260.
[24] Venugopal R, Lin PI, Liu CC, Chen YT. J Am Chem Soc 2005;127:11262.
[25] Jeong U, Xia Y, Yin Y. Chem Phys Lett 2005;416:246.
[26] Wang ZY, Zhang LD, Ye CH, Fang XS, Xiao ZD, Kong MG. J Nanosci Nanotechnol 2005;5:2088.
[27] Ma C, Wang ZL. Adv Mater 2005;17:2635.
[28] Thurn-Albrecht T, Schotter J, Kastle GA, Emley N, Shibauchi T, Krusin-Elbaum L, et al. Science 2000;290:2126.

[29] Cornelissen JJLM, Van Heerbeek R, Kamer PCJ, Reek JNH, Sommerdijk NAJM, Nolte RJM. Adv Mater 2002;14:489.
[30] Cavalli S, Popescu DC, Tellers EE, Vos MRJ, Pichon BP, Overhand M, et al. Angew Chem Int Ed 2006;45:739.
[31] Muniz G, Banerjee IA, Yu L, Djalali R, Chen Y-F, Matsui H. PMSE Preprints 2005;92:590.
[32] Djalali R, Chen Y-F, Matsui H. J Am Chem Soc 2002;124:13660.
[33] Adelung R, Aktas OC, Franc J, Biswas A, Kunz R, Elbahri M, et al. Nat Mater 2004;3:375.
[34] Yang Q, Tang K, Wang C, Qian Y, Zhang S. J Phys Chem B 2002;106:9227.
[35] Zhan J, Yang X, Wang D, Li S, Xie Y, Xia Y, et al. Adv Mater 2000;12:1348.
[36] Xie Y, Qiao ZP, Chen M, Liu XM, Qian YT. Adv Mater 1999;11:1512.
[37] Niu H, Zhang L, Gao M, Chen Y. Langmuir 2005;21:4205.
[38] Yang C-S, Awschalom DD, Stucky GD. Chem Mater 2002;14:1277.
[39] Zhang X-D, Jin J, Yang W-S, Fu L-S, Zhang H-J, Li T-J. Huaxue Xuebao 2002;60:532.
[40] Tian M, Li P-C, Yang W-S. Fenzi Kexue Xuebao 2002;18:75.
[41] Zhang M, Drechsler M, Müller AHE. Chem Mater 2004;16:537.
[42] Zhang M, Breiner T, Mori H, Müller AHE. Polymer 2003;44:1449.
[43] Deng Z, Cao L, Tang F, Zou B. J Phys Chem B 2005;109:16671.
[44] Clay RT, Cohen RE. Supramol Sci 1998;5:41.
[45] Zhang M, Teissier P, Krekhova M, Cabuil V, Müller AHE. Prog Colloid Polym Sci 2004;126:35.
[46] Achermann M, Petruska MA, Crooker SA, Klimov VI. J Phys Chem B 2003;107:13782.
[47] Artemyev MV, Woggon U, Jaschinski H, Gurinovich LI, Gaponenko SV. J Phys Chem B 2000;104:11617.
[48] Artemyev MV, Bibik AI, Gurinovich LI, Gaponenko SV, Woggon U. Phys Rev B Condens Matter 1999;60:1504.
[49] Kagan CR, Murray CB, Nirmal M, Bawendi MG. Phys Rev Lett 1996;76:1517.
[50] Kagan CR, Murray CB, Bawendi MG. Phys Rev B Condens Matter 1996;54:8633.
[51] Scholes GD. Ann Rev Phys Chem 2003;54:57.
[52] Hull K, Grebinski J, Protasenko V, Kuno M. Abstracts of papers, 229th ACS National Meeting, San Diego, CA, United States, March 13–17, 2005; PHYS.